

# Metamaterial photonic funnels for subdiffraction light compression and propagation

Alexander A. Goyadinov and Viktor A. Podolskiy\*

Physics Department, Oregon State University, 301 Weniger Hall, Corvallis, Oregon 97331, USA

(Received 19 December 2005; published 12 April 2006)

We present waveguides with photonic crystal cores, supporting energy propagation in subwavelength regions with a mode structure identical to that in telecom fibers and develop an analytical description of light transmission through these systems. We design metamaterials for near-, mid-, and far-IR frequencies, and demonstrate  $\sim 10\cdots 30\%$  energy transfer to and from regions smaller than  $1/25$ th of the wavelength via the numerical solution of Maxwell equations. Both positive- and negative-refractive index light transmissions are shown. Our approach, although demonstrated here in circular waveguides for some specific frequencies, is easily scalable from optical to IR to THz frequency ranges, and can be realized in a variety of waveguide geometries. Our design may be used for ultra high-density energy focusing, nm-resolution sensing, near-field microscopy, and high-speed photonic computing.

DOI: [10.1103/PhysRevB.73.155108](https://doi.org/10.1103/PhysRevB.73.155108)

PACS number(s): 42.81.Qb, 42.25.Bs, 87.64.Xx

## I. INTRODUCTION

While light emission by atoms, molecules, quantum wells, quantum dots, and other quantum objects occurs from nm-sized regions, light propagation takes place on  $\mu\text{m}$ -wide (wavelength) scales. Such a huge *scale difference* introduces fundamental limitations on (i) the size of waveguiding structures and (ii) the efficiency of coupling between nano- and micro-domains. These limitations, in turn, restrict the resolution and sensitivity of near-field microscopes,<sup>1,2</sup> prevent fabrication of ultracompact all-optical processing circuits,<sup>3,4</sup> integrated optoelectronic devices<sup>5,6</sup> and other photonic systems. Conventional techniques for light manipulation in subwavelength areas include coaxial cables,<sup>7</sup> anisotropic resonant or magnetic materials,<sup>8</sup> and plasmonic waveguides.<sup>9,10</sup> The first two designs, while successfully used in GHz frequencies, face extreme fabrication challenges in THz to optical domains. Moreover, the performance of all resonant systems, including magnetic metamaterials is strongly limited by resonant material absorption.<sup>8,11</sup> Plasmonic waveguides, although they can be used to transfer radiation to nm-sized regions,<sup>9,10</sup> have mode structure fundamentally different from the one in dielectric fibers.

Here we present a class of compact, nonmagnetic, non-resonant waveguides, capable of effective transfer of *free-space* radiation to, from, and in subwavelength regions. Our approach, although demonstrated here in circular waveguides for some specific frequencies, is easily scalable from optical to IR to THz frequency ranges, and can be realized in a variety of waveguide geometries.

## II. WAVE PROPAGATION IN WAVEGUIDES WITH ISOTROPIC CORES

The wave propagation in the confined spaces has some universal, design-independent properties. Specifically, the electromagnetic radiation in any waveguide forms a series of system-specific waves: *waveguide modes*. The wave vector of each mode in the direction of mode propagation  $k_z$  is

related to the frequency through the following dispersion relation:<sup>9,11–13</sup>

$$k_z^2 = \epsilon\nu \frac{\omega^2}{c^2}, \quad (1)$$

where  $\epsilon$  and  $\nu$  are mode-specific propagation constants. In waveguides with nonmagnetic isotropic homogeneous cores  $\epsilon$  is the dielectric permittivity of the core, and the parameter  $\nu = 1 - \frac{\pi^2 m^2 c^2}{\epsilon R^2 \omega^2}$  is related to the frequency  $\omega$ , the speed of light in the vacuum  $c$ , the mode confinement radius  $R$ , and a generally noninteger mode number  $m$  ( $|m| \geq 1$ ). The phase velocity of the mode is given by the effective index of refraction  $n = k_z c / \omega = \pm \sqrt{\epsilon\nu}$ .

The mode propagation is possible only when  $n^2 = \epsilon\nu > 0$ . For the waveguide with an isotropic homogeneous core, this condition is equivalent to  $\epsilon > 0$ ,  $\nu > 0$ ;  $n > 0$ . Thus, there exists a minimal critical radius of a waveguide supporting at least one confined propagating mode,  $R_0 \approx \pi c / (\omega \sqrt{\epsilon}) = \lambda / (2\sqrt{\epsilon})$ . The appearance of such a critical radius is in fact a manifestation of one of the fundamental laws of nature—diffraction limit. The systems with  $R < R_0$ , formally described by  $\epsilon > 0$ ,  $\nu < 0$ , reflect almost all incoming free-space-like radiation,<sup>1,14</sup> and are not suitable for energy transfer into subwavelength areas.

The waveguide properties can be controlled by either changing the mode structure (modifying the parameter  $m$ ), or by varying the waveguide core material (modifying the parameter  $\epsilon$ ). The majority of modern subwavelength optical waveguides<sup>7,10,15</sup> implement the former technique, and make use of the special type of modes at the metal-dielectric interfaces, known as surface waves, which formally correspond to  $m^2 < 0$ . The use of surface waves to adiabatically transfer radiation to nm-regions has been proposed in Ref. 9. However, the spatial structure of surface modes is fundamentally different from that of free-space waves and telecom fiber modes. This structural difference requires nontrivial coupling mechanisms to convert the radiation from free-space to sur-

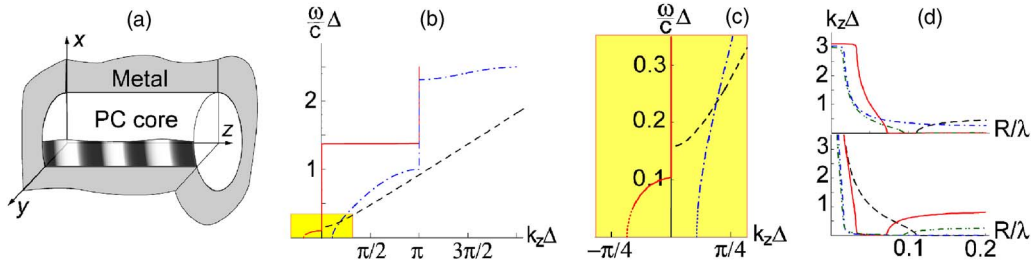


FIG. 1. (Color online) (a) Schematic geometry of a waveguide with a PC core. (b,c) Unfolded dispersion diagram of the  $TM_{01}$  mode in three different waveguides; material dispersion and absorption is neglected;  $a_1 = a_2$ . Black dashed line: Si core; note the frequency cutoff at  $|k_z\Delta| = 1/n$  corresponding to the diffraction limit; this behavior is similar to that of TE modes in PC structures described in the text. Blue dash-dot line:  $n > 0$  mode in SiC-Si PC. Red solid line:  $n < 0$  mode in an Ag-Si system. Inset shows the effective-medium  $|k_z\Delta| \ll 1$  region [highlighted area in (b) and (c)]; low-frequency regime [dotted region in (c)] is not realizable in nature since  $\epsilon(\omega \rightarrow 0)$  has to be positive.<sup>11</sup> (d) Confined mode propagation in PC waveguides. Absolute values of real (upper graph) and imaginary (lower graph) parts of the wave vector are shown for the  $TM_{01}$  mode in the Si-core (black dashed), and Ag-Si (red solid), Si-SiC (blue dash-dotted), and InGaAs-AllnAs (green dash-dot-dotted) PC structures (see text).

face waves, typically associated with substantial coupling losses.<sup>11,15,16</sup>

### III. SUBDIFFRACTION LIGHT PROPAGATION IN FIBERS WITH ANISOTROPIC METAMATERIAL CORES

Here we present an alternative approach to compress and propagate the radiation below the free-space diffraction limit. Instead of changing the structure of the modes, we propose to change the waveguide itself. We use a *periodic array* of thin dielectric ( $\epsilon > 0$ ) and “metallic” ( $\epsilon < 0$ ) layers [one-dimensional (1D) photonic crystal (PC)] as a *metamaterial waveguide core* [Fig. 1(a)]. Note that in contrast to previously proposed GHz systems,<sup>8</sup> our design relies neither on resonance nor on magnetism.

In the case of PC layers perpendicular to the direction of mode propagation considered here, all modes of the system can be separated into two fundamentally different groups. The modes in the first group, known as TE waves, have their electric ( $\mathbf{E}$ ) vector parallel to the layers, the modes in the second group, TM waves, have their magnetic ( $\mathbf{H}$ ) vector parallel to the layers. Similar to the case of a homogeneous waveguide described above, the frequency and wave vector of a wave in a PC-core fiber can be related through the dispersion relation:

$$\cos(k_z\Delta) = \cos(k_1a_1)\cos(k_2a_2) - \gamma \sin(k_1a_1)\sin(k_2a_2), \quad (2)$$

where  $a_1$  and  $a_2$  are the thicknesses of the layers in the PC,  $\epsilon_1 > 0$ , and  $\epsilon_2 < 0$  are their permittivities,  $k_1^2 = \epsilon_1\omega^2/c^2 - \pi^2m^2/R^2$ ,  $k_2^2 = \epsilon_2\omega^2/c^2 - \pi^2m^2/R^2$ ,  $\Delta = a_1 + a_2$ , and the parameter  $\gamma$  is equal to  $\gamma_{TE} = \frac{1}{2}\left(\frac{k_1}{k_2} + \frac{k_2}{k_1}\right)$  and  $\gamma_{TM} = \frac{1}{2}\left(\frac{\epsilon_2k_1}{\epsilon_1k_2} + \frac{\epsilon_1k_2}{\epsilon_2k_1}\right)$  for TE and TM modes, respectively.<sup>17</sup>

The case when the period of the system is much smaller than the wavelength [ $|k_1a_1| \ll 1$ ,  $|k_2a_2| \ll 1$  and  $|k_z(a_1 + a_2)| \ll 1$ ] is of a special interest for our design. In this limit Eq.

(2) becomes identical to Eq. (1) with polarization-specific propagation parameters  $\epsilon$  and  $\nu$ , given by

$$\begin{aligned} \epsilon &= \epsilon_{PC}^{TM} = \epsilon_{PC}^{TE} = \frac{a_1\epsilon_1 + a_2\epsilon_2}{a_1 + a_2}, \\ \nu_{PC}^{TM} &= 1 - \frac{a_1\epsilon_2 + a_2\epsilon_1}{\epsilon_1\epsilon_2(a_1 + a_2)} \frac{\pi^2m^2c^2}{R^2\omega^2}, \\ \nu_{PC}^{TE} &= 1 - \frac{1}{\epsilon_{PC}^{TE}} \frac{\pi^2m^2c^2}{R^2\omega^2}. \end{aligned} \quad (3)$$

In a way, the PC core plays the role of a homogeneous but anisotropic uniaxial metamaterial with its optical axis parallel to the direction of mode propagation.<sup>13</sup> This effective medium response of PC structure is almost unaffected by material periodicity and therefore is highly tolerable to fabrication defects.

The propagation of TE modes in PC waveguides is completely analogous to the propagation in isotropic systems described earlier. In contrast to this behavior, the PC structure can support TM waves in two fundamentally different regimes. The first regime, described by  $\epsilon_{PC}^{TM} > 0$ ;  $\nu_{PC}^{TM} > 0$  corresponds to  $n = \sqrt{\epsilon\nu} > 0$ , while the second one,  $\epsilon_{PC}^{TM} < 0$ ;  $\nu_{PC}^{TM} < 0$  describes a  $n = -\sqrt{\epsilon\nu} < 0$  case<sup>13,18</sup> unachievable in conventional fiber- and plasmonic-waveguides.<sup>2,7,9,10,12,15</sup>

Both  $n > 0$  and  $n < 0$  structures may support wave propagation in highly-confined areas (Fig. 1). Indeed, the refractive index in substantially thin ( $R \ll \lambda$ ) strongly anisotropic systems  $\propto 1/R$ . The decrease in  $R$  is accompanied by a decrease of internal wavelength  $\lambda/|n|$ , virtually eliminating the diffraction limit for TM waves in proposed structures. Furthermore, the PC waveguides with different refractive indices can be combined together, opening the door for the effective phase manipulation of light propagating in highly-confined areas. The possibility of such a versatile light management on nanoscale is one of the main points of this work.

To illustrate the proposed design and its scalability we calculate the light propagation through PC waveguides with

(i) 100-nm-thick layers of SiC and Si with operating wavelength  $\lambda=11\ \mu\text{m}$ , (ii) 15-nm-thick layers of Ag and Si with operating wavelength  $\lambda=1.2\ \mu\text{m}$ , and (iii) 75 nm-thick InGaAs layers doped with electrons to  $10^{19}\ \text{cm}^{-3}$ , and 150 nm AlInAs barriers with operating wavelength  $\lambda=20\ \mu\text{m}$ . (Fabrication of these structures is accessible through standard MOCVD, *e*-beam writing, or MBE techniques; see Refs. 10, 19, and 20 and references therein). The first of these structures has  $n>0$ , while the latter two systems correspond to  $n<0$ .

In Fig. 1 we illustrate mode propagation in cylindrical PC systems and compare it to the modes in waveguide with a homogeneous Si core.<sup>21</sup> The appearance of the cutoff radius in isotropic systems, along with energy propagation in sub-wavelength metamaterial-waveguides is clearly seen. It is interesting to note the difference between the cutoff properties of modes in  $n>0$  and  $n<0$  PCs. The  $n>0$  systems are only affected by material inhomogeneity (see below), while  $n<0$  modes require  $\nu<0$  and therefore propagate only in sufficiently thin waveguides.<sup>13</sup>

#### IV. MODE COMPRESSION IN PHOTONIC FUNNELS

The self-adjustment of PC waveguide modes to the waveguide size, accompanied by compatibility between the mode structure in PC waveguides, telecom fibers, and free-space makes the PC systems ideal candidates for effective energy transfer between macroscopic wave-propagation systems and nanoscale objects. In these coupling structures, called *photonic funnels*, the size of the PC waveguides gradually varies along the direction of mode propagation, squeezing the light into nm-sized areas much like a conventional funnel squeezes water into a thin bottleneck, which is another main point of this work.

The efficiency of energy compression in photonic funnels can be related to an adiabaticity parameter  $\delta = \left| \frac{d(1/k_z)}{dz} \right|$ , that defines the reflection by the funnel structure,<sup>9,11</sup> and absorption in the system. Increase of the funnel's length typically reduces reflection loss, but increases absorption.

In Figs. 2 and 3 we illustrate the light propagation in PC-based photonic funnels with metamaterial cores described above. Although our design does not impose any limitations on the waveguide geometry or waveguide boundary material, here we use conical waveguides with perfectly conducting metallic walls (see Ref. 22) and circular cores, having adiabaticity parameters  $\delta \sim 0.1 \cdots 0.3$ , and defer the optimization of a photonic funnel geometry to future work.

To compute the light propagation in conical structures, we represent each structure by an array of cylindrical segments (in a way, this approach also accounts for the effects related to finite roughness of waveguide walls, unavoidable in any experiment). The typical radius step in our calculations is  $10^{-3}\lambda$ . We then represent the field in each cylindrical segment as a series of modes of a circular waveguide. We use Eqs. (2) and (3) to calculate a mode propagation in each segment. In these calculations we use experimental values of permittivities for Ag, Si, SiC, and AlGaAs<sup>23</sup> and use the Drude approach to describe doped InGaAs.<sup>11</sup> Finally, we use the boundary conditions to relate the modes in one segment

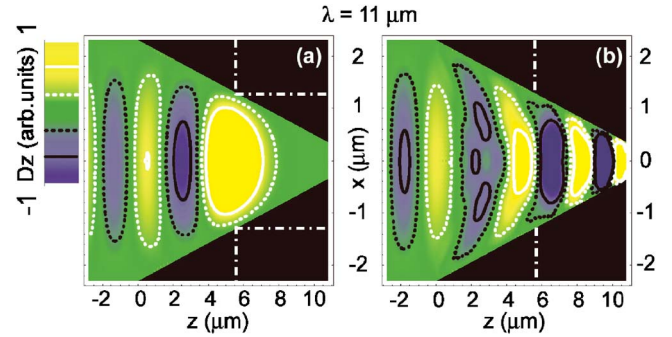


FIG. 2. (Color online)  $\text{TM}_{01}$  mode propagation ( $\lambda=11\ \mu\text{m}$ ) from cylindrical Si waveguide ( $z<0$ ) to a conical one with circular core;  $D_z$  component shown; solid white, dashed white, dashed black, and solid black contours correspond to  $D_z$  values of 0.75, 0.25,  $-0.25$ , and  $-0.75$ , respectively (see scale); (a) Si core structure. Note the reflection from the point where the radius reaches cutoff value  $R_0 \approx 1.2\ \mu\text{m}$  (dash-dotted lines). Only  $10^{-10}$  of energy is transmitted from  $R=2.3\ \mu\text{m}$  to  $R=0.35\ \mu\text{m} \sim \lambda/31$ . This behavior is similar to that in tips of near-field microscopes.<sup>1,2</sup> (b) Field concentration in Si-SiC PC funnel described in the text: 13% of energy is transmitted to  $R=0.35\ \mu\text{m}$ , 16% is reflected back to the Si ( $z<0$ ) waveguide. Note the dependence of the internal wavelength on the radius.

to the modes in the neighboring segment, solving the problem of wave propagation through a photonic funnel.

In Fig. 2 we demonstrate the perspectives of photonic funnels by comparing the energy propagation through mid-IR PC waveguide with positive refraction described above to the propagation through the Si-core structure with identical geometry.<sup>21</sup> As expected, despite almost adiabatic radius compression, the energy in Si-core system reflects from the point corresponding to the cutoff radius of about  $1.2\ \mu\text{m}$ . In contrast to this behavior, the PC system effectively compresses energy, and the propagation in the structure with radius as small as  $0.35\ \mu\text{m} \approx \lambda/30$  is clearly seen. This PC provides a solution to the fundamental problem of coupling to the subwavelength domain, and allows transferring 13% of energy, which is  $10^9$  times better than its Si counterpart.

The effective energy transfer across multiple scales in “negative-refraction” near- and far-IR PC systems is shown in Fig. 3. It is clearly seen that the mode propagation in  $n<0$  systems is qualitatively similar to the one in  $n>0$  waveguides. However, the existence of the maximum cutoff radius may require a radius mismatch between the “feeder” and “funnel” waveguides, as illustrated in Fig. 3. Our calculations suggest that the Ag-Si system may be used to transfer more than 20% of energy to the near-field zone. We expect that this number can be further optimized by reducing the wave reflection (currently 21%). The same system may be used to transfer the energy from nm-sized spots to far-field zone. Our results demonstrate 11% energy transmission in the  $\text{TM}_{11}$  mode [see Fig. 3(b)]. The performance of the far-IR system is similar to that of an Si-Ag composite [Fig. 3(c)].

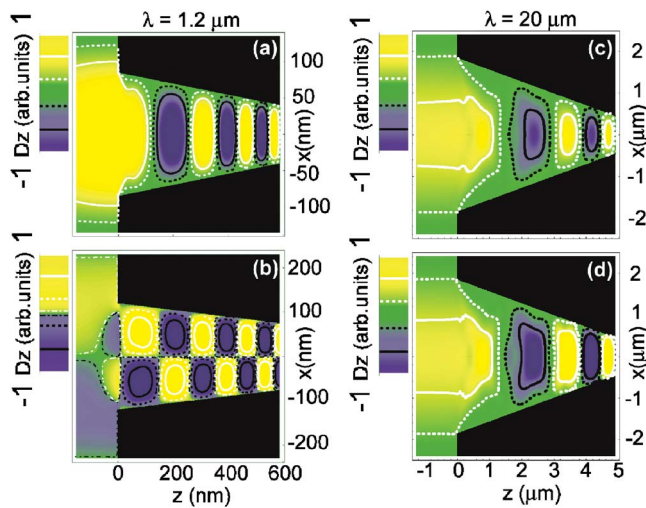


FIG. 3. (Color online) Negative refractive index systems;  $D_z$  component shown; solid white, dashed white, dashed black, and solid black contours correspond to  $D_z$  values of 0.75, 0.25,  $-0.25$ , and  $-0.75$ , respectively (see scales). (a and b) Homogeneous Si waveguide ( $z < 0$ ) coupled to Ag-Si PC core cone as described in the text;  $\lambda = 1.2 \mu\text{m}$ , (a)  $\text{TM}_{01}$  mode transfer from Si to a PC structure: 24% of energy is transmitted from  $R = 135 \text{ nm}$  to  $R = 40 \text{ nm} \sim \lambda/26$ , 21% is reflected back to Si waveguide. (b)  $\text{TM}_{11}$  mode transfer from the PC system ( $z > 0$ ) to Si waveguide: 11% of energy is transferred from  $R = 75 \text{ nm} \sim \lambda/16$  to  $R = 230 \text{ nm}$ , 13% is reflected back. (c) and (d)  $\text{TM}_{01}$  energy transfer from AllnAs waveguide ( $z < 0$ ) to passive (c) and active (d) InGaAs-AllnAs PC-core;  $\lambda = 20 \mu\text{m}$ . The passive structure transmits 6% of radiation from  $R = 2.4 \mu\text{m}$  to  $R = 0.45 \mu\text{m} \sim \lambda/44$ . The material gain in active system ( $\epsilon_{\text{AllnAs}} \approx 10 - i$ ) compensates for losses in the funnel structure and yields energy in  $R = 0.45 \mu\text{m}$  to be 112% of the incident one. Similar to Fig. 2, the internal wavelength is proportional to  $R$ .

### V. LIMITATIONS OF THE PROPOSED APPROACH AND CONCLUDING REMARKS

The performance of the PC-based waveguides is limited by the PC microstructure, and by material absorption. The

former introduces implicit inhomogeneity scale (PC period), where the “effective medium” approximation [Eq. (3)] breaks down. The spatial dispersion, associated with field inhomogeneities on such a scale, leads to the mode cutoff and prohibits the mode propagation when the radius of a waveguide becomes smaller than the PC period. The appearance of such a cutoff is shown in Fig. 1(c).

Material losses, on the other hand, lead to energy attenuation and limit the length of passive photonic funnels to  $\sim 10\lambda$  which is acceptable for the majority of applications of these systems: near-field tips, ultracompact detectors, wires in all-optical circuits, etc. This limitation is not applicable to waveguides with active cores. Indeed, material absorption can be substantially reduced, eliminated, or even reversed by implementing a gain medium into  $\epsilon > 0$  regions of PC.<sup>24</sup> We illustrate this approach in Fig. 3(d) by adding gain into the AllnAs part of the far-IR structure, which can be realized via quantum cascade technology.<sup>19</sup>

Finally, we note that operating frequency of the photonic funnels described here can be changed from optical, to near-IR, to far-IR, to THz domain by varying the PC composition and periodicity. The PC-based waveguides may be used in ultracompact all-optical and electro-optical devices, near-field microscopy, and other applications requiring effective subdiffraction and cross-scale energy transfer, as well as in a variety of nonlinear optical applications<sup>20</sup> in positive- and negative-index materials since the energy compression and corresponding enhancement of the local field will result in the strong enhancement of nonlinear field moments.

### ACKNOWLEDGMENTS

The authors would like to thank E. Mishchenko and M. Stockman for fruitful discussions. This research has been partially supported by the General Research Fund (Oregon State University).

\*Electronic address: viktor.podolskiy@physics.oregonstate.edu

<sup>1</sup>A. Lewis, H. Taha, A. Strinkovski, A. Manevitch, A. Khatchaturian, R. Dekhter, and E. Ammann, *Nat. Biotechnol.* **21**, 1378 (2003).

<sup>2</sup>E. Betzig, J. K. Trautman, T. D. Harris, J. S. Weiner, and R. L. Kostelak, *Science* **251** 1468, (1991).

<sup>3</sup>S. F. Mingaleev and Y. S. Kivshar, *J. Opt. Soc. Am. B* **19** 2241 (2002).

<sup>4</sup>M. F. Yanik, S. Fan, M. Soljčić, and J. D. Joannopoulos, *Opt. Lett.* **28** 2506 (2003).

<sup>5</sup>D. Walba, *Science* **270** 250 (1995).

<sup>6</sup>Q. Xu, B. Schmidt, S. Pradhan, and M. Lipson, *Nature (London)* **435**, 325 (2005).

<sup>7</sup>H. G. Frey, F. Keilmann, A. Kriele, and R. Guckenberger, *Appl. Phys. Lett.* **81**, 5030 (2002); A. Kramer, F. Keilmann, B. Knoll, and R. Guckenberger, *Micron* **27**, 413 (1996).

<sup>8</sup>R. Marques, J. Martel, F. Mesa, and F. Medina, *Phys. Rev. Lett.* **89** 183901 (2002); J. D. Baena, L. Jelinek, R. Marques, and F.

Medina, *Phys. Rev. B* **72**, 075116 (2005); P. A. Belov and C. R. Simovski, *Phys. Rev. E* **72**, 036618 (2005); S. Hrabar, *IEEE Trans. Antennas Propag.* **53**, 110 (2005); A. Alu and N. Enggelta, *IEEE Trans. Microwave Theory Tech.* **52**, 199 (2004).

<sup>9</sup>M. I. Stockman, *Phys. Rev. Lett.* **93**, 137404 (2004).

<sup>10</sup>S. A. Maier, P. G. Kik, H. A. Atwater, S. M. Meltzer, E. Harel, B. E. Koel, and A. G. Requicha, *Nature (London)* **2**, 229 (2003); P. G. Kik, S. A. Maier, and H. A. Atwater, *Phys. Rev. B* **69**, 045418 (2004); A. Karalis, E. Lidorikis, M. Ibanescu, J. D. Joannopoulos, and M. Soljčić, *Phys. Rev. Lett.* **95**, 063901 (2005); S. I. Bozhevolnyi, V. S. Volkov, and K. Leosson, *ibid.* **89**, 186801 (2002).

<sup>11</sup>L. D. Landau, E. M. Lifshitz, and L. P. Pitaevskii, *Course of Theoretical Physics*, 2nd ed., (Reed, New Zealand, 1984) Vol. 8.

<sup>12</sup>J. D. Joannopoulos, R. D. Meade, and J. N. Winn, *Photonic Crystals: Molding the Flow of Light*, (Purdue Press, Indiana, 1995); J. C. Knight, J. Broeving, T. A. Birks, and P. J. Russel, *Science* **282**, 1476 (1998); Y. Fink, J. N. Winn, S. Fan, C. Chen, J.

- Michel, J. D. Joannopoulos, and E. L. Thomas, *ibid.* **282**, 1679 (1998).
- <sup>13</sup>V. A. Podolskiy and E. E. Narimanov, *Phys. Rev. B* **71**, 201101(R) (2005); R. Wangberg, J. Elser, E. E. Narimanov, and V. A. Podolskiy, *J. Opt. Soc. Am. B* **23**, 498 (2006).
- <sup>14</sup>An exponentially small part of radiation can penetrate through the subcritical waveguide of finite length in a manner similar to the light transmission through thin metallic film.
- <sup>15</sup>A. Bouhelier, J. Renger, M. R. Beversluis, and L. Novotny, *J. Microsc.* **210** 220 (2002).
- <sup>16</sup>F. Demming, A. v-d Lieth, S. Klein, and K. Dickmann, *Adv. Funct. Mater.* **11**, 198 (2001).
- <sup>17</sup>P. Yeh, A. Yariv, and C. Hong, *J. Opt. Soc. Am.* **67**, 423 (1977).
- <sup>18</sup>V. G. Veselago, *Sov. Phys. Usp.* **10**, 509 (1968); J. B. Pendry *Phys. Rev. Lett.* **85**, 3966 (2000).
- <sup>19</sup>C. Gmachl, F. Capasso, E. E. Narimanov, J. U. Nckel, A. D. Stone, J. Faist, D. L. Sivco, and A. Y. Cho, *Science* **280**, 1556 (1998); M. Troccoli, A. Belyanin, F. Capasso, E. Cubukcu, D. L. Sivco, and A. Y. Cho, *Nature (London)* **433**, 845 (2005).
- <sup>20</sup>N. N. Lepeshkin, A. Schweinsberg, R. S. Bennink, and R. W. Boyd, *Phys. Rev. Lett.* **93**, 123902 (2004); R. S. Bennink, Y. Yoon, R. W. Boyd, and J. E. Sipe, *Opt. Lett.* **24**, 1416 (1999).
- <sup>21</sup>Since Si has one of the largest dielectric constants of all transparent natural materials, isotropic Si-core waveguides in a sense correspond to the “minimum achievable” cutoff radius.
- <sup>22</sup>At IR frequencies, Ag, Au, and Al have dielectric permittivities at least an order of magnitude larger than the effective permittivities of our systems, and therefore are adequately described by “perfectly conducting metal” boundary conditions. The quantitatively weak effect of finite wall conductance can be treated using standard perturbation techniques see Ref. 13.
- <sup>23</sup>*The Handbook of Optical Constants of Solids*, edited by E. Palik (Academic Press, New York, 1997).
- <sup>24</sup>S. A. Ramakrishna and J. B. Pendry, *Phys. Rev. B* **67**, 201101(R) (2003).